Using t→bb[over ¯]c to search for new physics

Ken Kiers, Tal Knighton, David London, Matthew Russell, Alejandro Szynkman, and Kari Webster

Phys. Rev. D **84**, 074018 — Published 13 October 2011

DOI: 10.1103/PhysRevD.84.074018

UdeM-GPP-TH-11-200

Using $t \to b\bar{b}c$ to Search for New Physics

Ken Kiers,[1,*] Tal Knighton,[1,†] David London,[2,‡] Matthew Russell,[1,§] Alejandro Szynkman,[2,3,¶] and Kari Webster[1,**]

[1]*Physics and Engineering Department, Taylor University, 236 West Reade Ave., Upland, IN 46989, USA*

[2]*Physique des Particules, Université de Montréal, C.P. 6128, succ. centre-ville, Montréal, QC, Canada H3C 3J7*

[3]*IFLP, CONICET – Dpto. de Física, Universidad Nacional de La Plata, C.C. 67, 1900 La Plata, Argentina*

Abstract

We consider new-physics (NP) contributions to the decay $t \to b\bar{b}c$. We parameterize the NP couplings by an effective Lagrangian consisting of 10 Lorentz structures. We show that the presence of NP can be detected through the measurement of the partial width. A partial identification of the NP can be achieved through the measurements of a forward-backward-like asymmetry, a top-quark-spin-dependent asymmetry, the partial rate asymmetry, and a triple-product asymmetry. These observables, which vanish in the standard model, can all take values in the 10-20% range in the presence of NP. Since $|V_{tb}V_{cb}| \simeq |V_{ts}V_{cs}|$, most of our results also hold, with small changes, for $t \to s\bar{s}c$.

*Electronic address: knkiers@taylor.edu

†Electronic address: tal_knighton@taylor.edu

‡Electronic address: london@lps.umontreal.ca

§Electronic address: russell2@math.rutgers.edu; Current address: Department of Mathematics – Hill Center, Rutgers, The State University Of New Jersey, 110 Frelinghuysen Rd., Piscataway, NJ 08854-8019, USA.

¶Electronic address: szynkman@fisica.unlp.edu.ar

**Electronic address: kari_webster@taylor.edu

I. INTRODUCTION

On the whole, measurements of observables in the B system agree with the Standard Model (SM). However, some cracks have started to appear. There are now several quantities whose measured values differ from the predictions of the SM. Although these disagreements are not statistically significant – they are typically at the level of $\sim 2\sigma$ – they are intriguing since there are a number of different B decays and effects involved, and they all appear in $b \to s$ transitions. Because of this, there have been numerous papers examining new-physics (NP) flavour-changing neutral-current (FCNC) contributions to the various $b \to s$ processes. These analyses have been performed in the context of specific NP models, or model-independently.

In general, such NP can also contribute to FCNC processes involving the top quark. This has been looked at, though much less so than in B decays. However, given that the LHC will produce a large number of top quarks and will be able to measure flavour-changing t decays, it is important to explore the possibility of NP contributions to FCNCs in the top sector. In the past, analyses have focused on rare top decays such as $t \to cV$ ($V = g, \gamma, Z$) and $t \to ch$ [1, 2]. Other top decays where NP effects have been examined include $t \to b\tau^+\nu$ [2–9] and $t \to W^+ d_k$ [10].

In this paper we examine the decay $t \to b\bar{b}c$. In the SM, this decay occurs at tree level, via $t \to bW \to b\bar{b}c$. On the other hand, because it involves the small element V_{cb} ($\simeq 0.04$) of the Cabibbo-Kobayashi-Maskawa (CKM) quark mixing matrix, the amplitude for this process is also rather small, and is therefore quite sensitive to NP. For example, there could be NP FCNC contributions to this decay in models with a charged Higgs boson [2], or via $t \to X^0 c \to b\bar{b}c$, where X^0 corresponds to some neutral particle (such as a Z' or a non-SM Higgs boson). Such FCNC processes could interfere with the SM process, leading to observable consequences, even if the intermediate NP particle were heavier than the top quark. Rather than restricting our attention to any one particular model, we examine NP contributions to $t \to b\bar{b}c$ model-independently (i.e., using an effective Lagrangian).

Our model-independent treatment of $t \to b\bar{b}c$ takes into account the effects of the 10 possible four-Fermi operators. These operators contribute to both CP-conserving and CP-violating observables. For the CP-even observables, we consider the CP-averaged partial width, a forward-backward-like asymmetry, and an asymmetry that depends on the spin of

the top quark. For the CP-odd observables, we note that the decay $t \to b\bar{b}c$ is dominated by one amplitude in the SM; i.e., there is only one weak phase involved. As such, all CP-violating asymmetries are very suppressed in the SM, so the observation of a non-zero asymmetry would be a smoking-gun signal of NP. In this paper, we discuss two types of CP-odd asymmetries: the partial-rate asymmetry (PRA) and a triple-product asymmetry (TPA).

PRAs require a strong phase in order to be non-zero. Strong phases can arise due to gluon exchange, but it is expected that such phases will be small since the energies involved are so large. Another source of a strong phase is the width of the W. In our calculation, we ignore QCD-based strong phases and assume that the required strong phase is due entirely to the width of the W. This means that only SM-NP interference can lead to a PRA. On the other hand, in contrast with PRAs, TPAs do not require a strong phase in order to be non-zero. Thus, NP-NP interference terms can give rise to TPAs. As we will see, TPAs generated by SM-NP interference tend to be small, but NP-NP TPAs can be large. These are particularly interesting.

We show that the measurement of the partial width by itself can reveal the presence of NP. However, if the NP exists, we will want to know its identity, i.e., which of the 10 operators is responsible, and the partial width measurement does not give us this information. In order to do this, it is necessary to measure the other quantities mentioned above. Since the various observables depend differently on the operators, the knowledge of their sizes will give us an idea of which NP operators are present. This will allow us in turn to deduce which model(s) might be responsible for the observed effects.

Although we confine our attention to $t \to b\bar{b}c$ in this work, we note that most of our results are easily transferable to $t \to s\bar{s}c$ by the replacement $\left(b, \bar{b}\right) \to (s, \bar{s})$ in Feynman diagrams and expressions. Since $|V_{tb}V_{cb}| \simeq |V_{ts}V_{cs}|$, the branching ratio for $t \to s\bar{s}c$ is similar to that for $t \to b\bar{b}c$, and the two processes would apriori have similar sensitivities to NP effects. One difference between $t \to b\bar{b}c$ and $t \to s\bar{s}c$ is that the "CPT" correction to the PRA would be significant for $t \to s\bar{s}c$, whereas it is miniscule for $t \to b\bar{b}c$ (see the discussion in Sec. IV A and Appendix B).

The remainder of this paper is organized as follows. In Sec. II we write down the SM contribution to $t \to b\bar{b}c$, and also parameterize NP contributions to this decay in terms of an effective Lagrangian containing ten terms. In Sec. III (CP-even observables) we compute

the CP-averaged partial width for the decay under consideration, as well as a forward-backward-like asymmetry and an asymmetry based on the spin of the top quark. The latter two asymmetries are both constructed in such a way that they are zero within the context of the SM. We close this section with a brief numerical study, noting that the CP-even asymmetries could reasonably be of order 10's of percent. Section IV contains our analysis of two CP-odd observables – the partial rate asymmetry and the triple-product asymmetry. Section V concludes with a discussion of our results. Appendices A, B and C contain some technical details. In particular, Appendix B contains a discussion of results related to the CPT theorem, namely which vertex-type corrections must be considered in the calculation of PRAs in order not to violate CPT.

II. STANDARD MODEL AND NEW-PHYSICS CONTRIBUTIONS

In this section we parameterize the NP contributions to $t \to b\bar{b}c$ in terms of an effective Lagrangian. We then write down expressions for the SM and NP amplitudes. These expressions are used in following sections to determine various CP-even and CP-odd observables.

Figure 1(a) shows the Feynman diagram for the SM contribution to $t \to b\bar{b}c$. The resulting amplitude is given by,

$$\mathcal{M}_W \;=\; -2\sqrt{2}G_F m_W^2 V_{cb}V_{tb}\,(\overline{u}_b\gamma_\alpha P_L u_t)\;(\overline{u}_c\gamma_\beta P_L v_b)\left[-g^{\alpha\beta}G_T(q^2)\right], \tag{1}$$

where V is the CKM matrix. We work in the standard representation of the CKM matrix, in which V_{cb} and V_{tb} are both real. Note that colour indices have been suppressed. The expression in square parentheses is the W propagator, with $q = p_t - p_b = p_{\overline{b}} + p_c$, $G_T(q^2) = [q^2 - m_W^2 + i\epsilon_T(q^2)]^{-1}$ and $\epsilon_T(q^2) \simeq q^2\Gamma_W/m_W$, where $\Gamma_W \simeq 3G_F m_W^3/(2\sqrt{2}\pi)$.

(Note: throughout this paper we neglect the leptons' and light quarks' masses. However, if this not done, the W propagator is modified to

$$i\left[\left(-g^{\alpha\beta} + \frac{q^\alpha q^\beta}{q^2}\right)G_T(q^2) + \frac{q^\alpha q^\beta}{q^2}G_L(q^2)\right]\;, \tag{2}$$

where $G_L = [m_W^2 + i\epsilon_L(q^2)]^{-1}$. $\epsilon_T(q^2)$ and $\epsilon_L(q^2)$ are related to the transverse and longitudinal widths of the W [6], and they both depend on the quark masses. There has been considerable discussion in the literature regarding the correct form of the W propagator. (See, for example, Refs. [5–7, 11–15].) The above expression has been derived by performing

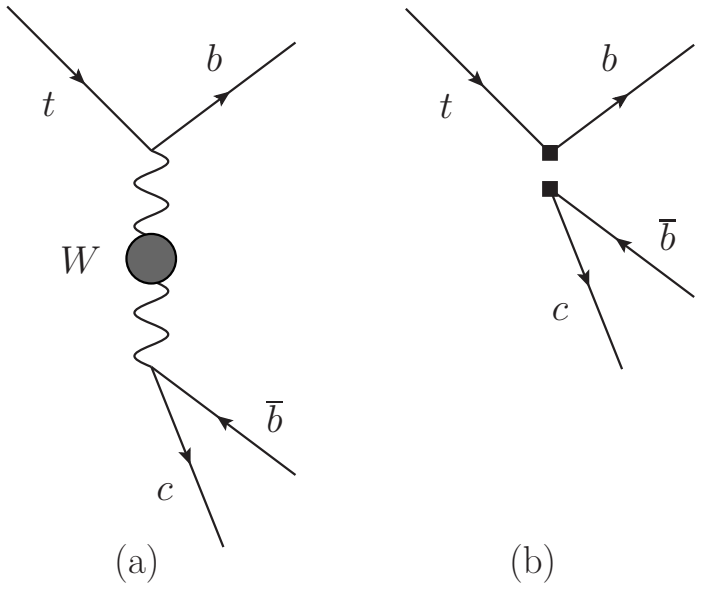

FIG. 1: Feynman diagrams for $t \to b\bar{b}c$. Diagram (a) shows the SM contribution. Diagram (b) shows the NP contributions in the effective theory. The NP contributions are assumed to have the same colour structure as that of the SM. See Appendix C for comments regarding the more general case.

a Dyson summation of the absorptive parts of the W self-energy diagrams in unitary gauge, with quarks and leptons in the loops. Some of the disagreement in the literature has focused on the form of G_L (see the brief discussion in Ref. [9], for example). Still, when all light masses are neglected, none of the observables in the present work depend on G_L. There seems to be broader agreement on the form for G_T in the literature, although many authors drop the q^2 dependence in ϵ_T. Finally, we should note that the Pinch Technique may be used to reorganize perturbative calculations – even those involving resonances – in such a way that results are explicitly gauge-invariant (see, for example, Ref. [15]). Rigorous application of the Pinch Technique to the problem at hand is beyond the scope of this work.)

We parameterize new-physics effects via an effective Lagrangian $\mathcal{L}_{\text{eff}} = \mathcal{L}^V_{\text{eff}} + \mathcal{L}^S_{\text{eff}} + \mathcal{L}^T_{\text{eff}}$, where,

$$\begin{aligned}\mathcal{L}^V_{\text{eff}} \;=\; \frac{g'^2}{M^2}\,\big\{&\mathcal{R}^V_{LL}\,\bar{b}\gamma_\mu P_L t\,\bar{c}\gamma^\mu P_L b + \mathcal{R}^V_{LR}\,\bar{b}\gamma_\mu P_L t\,\bar{c}\gamma^\mu P_R b \\ &+\mathcal{R}^V_{RL}\,\bar{b}\gamma_\mu P_R t\,\bar{c}\gamma^\mu P_L b + \mathcal{R}^V_{RR}\,\bar{b}\gamma_\mu P_R t\,\bar{c}\gamma^\mu P_R b\big\} + \text{h.c.},\end{aligned} \tag{3}$$

$$\mathcal{L}^S_{\rm eff} \;=\; \frac{g'^2}{M^2}\left\{\mathcal{R}^S_{LL}\,\bar{b}P_L t\,\bar{c}P_L b + R^S_{LR}\,\bar{b}P_L t\,\bar{c}P_R b \right.$$
$$\left. +\mathcal{R}^S_{RL}\,\bar{b}P_R t\,\bar{c}P_L b + \mathcal{R}^S_{RR}\,\bar{b}P_R t\,\bar{c}P_R b\right\} + \text{h.c.}, \tag{4}$$

$$\mathcal{L}^T_{\rm eff} \;=\; \frac{g'^2}{M^2}\left\{\mathcal{C}_T\,\bar{b}\sigma_{\mu\nu}t\,\bar{c}\sigma^{\mu\nu}b + i\,\mathcal{C}_{TE}\,\bar{b}\sigma_{\mu\nu}t\,\bar{c}\sigma_{\alpha\beta}b\,\epsilon^{\mu\nu\alpha\beta}\right\} + \text{h.c.} \tag{5}$$

In the above expressions, g' is assumed to be of order g, M is the NP mass scale and the $\mathcal{R}$ and $\mathcal{C}$ couplings may include weak (CP-violating) phases. For the Levi-Civita tensor, we adopt the convention $\epsilon^{0123} = +1$. The NP contributions to $t \to b\bar{b}c$ are illustrated in Fig. 1(b). Colour indices are not shown in the above expressions, but are assumed to contract in the same manner as those of the SM (i.e., $\bar{b}$ with t and $\bar{c}$ with b). In FCNC models – those with a flavour-changing neutral particle such as a Z' or a scalar – the colour indices would contract in the opposite manner (i.e., $\bar{c}$ with t and $\bar{b}$ with b). It is straightforward to incorporate colour-mismatched terms into the effective Lagrangian. This topic is discussed further in Appendix C.

It is useful to define

$$X^V_{LL} \equiv \left(\frac{g'}{g}\right)^2\left(\frac{m_W}{M}\right)^2\frac{\mathcal{R}^V_{LL}}{V_{tb}V_{cb}} = \frac{\sqrt{2}}{8G_F}\frac{g'^2}{M^2}\frac{\mathcal{R}^V_{LL}}{V_{tb}V_{cb}}\,, \tag{6}$$

and similarly for the other $\mathcal{R}$ and $\mathcal{C}$ couplings. In terms of the "X" parameters, we have the following expression for the NP contribution to $t \to b\bar{b}c$,

$$\mathcal{M}_{\rm NP} \;=\; 4\sqrt{2}G_F V_{cb}V_{tb}\left\{X^V_{LL}\,\overline{u}_b\gamma_\mu P_L u_t\,\overline{u}_c\gamma^\mu P_L v_b + \ldots\right\}. \tag{7}$$

To get a sense of the possible order of magnitude of the X couplings, note that, if $g' \sim 2g$ and $M \sim 500$ GeV, then $X^V_{LL} \sim 2.5 \times \mathcal{R}^V_{LL}$. Thus, X^V_{LL} could reasonably be assumed to be of order unity. In other words, the SM and NP contributions to $t \to b\bar{b}c$ can very well be about the same size. When computing the effect of NP on a particular observable, it is therefore important to include both the SM-NP interference and NP^2 pieces.

At present, there are no direct constraints on the X couplings. The precision measurements of V_{cb} place an indirect constraint via the loop diagram shown in Fig. 2. It is known that some care must be taken when attempting to incorporate terms from an effective Lagrangian into loop calculations [16]. Incorporating the diagram shown in Fig. 2, we find the following expression for the effective Lagrangian for $b \to c\ell\overline{\nu}$,

$$\mathcal{L}^{\rm SM+NP}_{\rm eff} \simeq -2\sqrt{2}\,G_F V_{cb}\left[\left(1+\zeta^V_{LL}\right)\bar{c}_L\gamma_\mu b_L + \zeta^V_{LR}\,\bar{c}_R\gamma_\mu b_R\right]\bar{\ell}_L\gamma^\mu\nu_L + \text{h.c.}, \tag{8}$$

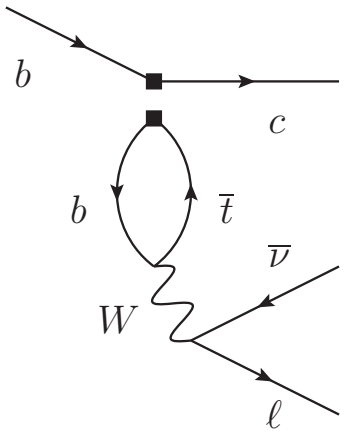

FIG. 2: Loop-level contribution of the NP operators to $b \to c\ell\overline{\nu}$. This contribution affects the measurement of V_{cb}.

in which we have dropped corrections of order $\mathcal{O}\left(m_b/m_t\right)$. Using the Feynman rules for the various vertices, and employing dimensional arguments, we estimate

$$\zeta^V_{LL(R)} \sim \frac{G_F m_t^2}{2\sqrt{2}\pi^2} \left(V_{tb}\right)^2 X^V_{LL(R)}. \tag{9}$$

Since semileptonic $b \to c$ transitions are used to determine V_{cb}, the experimental value of V_{cb} can be used to bound X^V_{LL} and X^V_{LR}. Let us first consider the X^V_{LL} term in Eq. (8), ignoring the X^V_{LR} term. The X^V_{LL} term has exactly the same structure as the SM term. Its effect is thus simply to multiply any inclusive or exclusive $b \to c\ell\overline{\nu}$ width by a factor of $\left[1 + 2\mathrm{Re}\left(\zeta^V_{LL}\right) + \left|\zeta^V_{LL}\right|^2\right]$. The current experimental value of V_{cb} is $V_{cb} = (40.6 \pm 1.3) \times 10^{-3}$ [17], implying a 6.4% uncertainty on V^2_{cb}. If we assume that the X^V_{LL} contribution to $b \to c\ell\overline{\nu}$ is hiding in the experimental uncertainty of V^2_{cb}, we find the bound,

$$\mathrm{Re}\left(X^V_{LL}\right) \lesssim 2.6, \tag{10}$$

in which we have neglected the quadratic contribution of ζ^V_{LL}, since it is small. Since X^V_{LR} is associated with the right-handed quark current in Eq. (8), its effect is process-dependent. For example, for $B \to D\ell\overline{\nu}$, the hadronic matrix element is only sensitive to the vector part of the hadronic current, so left-handed and right-handed couplings both have the same effect, and they can be absorbed in with the SM current [18]. For other modes, such as $B \to D^*\ell\overline{\nu}$, the right-handed and left-handed currents must be treated differently [18].

Since our expression in Eq. (9) is somewhat of an approximation in any case, we assume the same upper bound for X^V_{LR} as for X^V_{LL}, i.e.,

$$\mathrm{Re}\left(X^V_{LR}\right) \lesssim 2.6. \tag{11}$$

The NP operators considered in this work could contribute, via loops, to other observables as well. As an example, consider the decay $B \to \psi K_S$, which proceeds at tree-level in the SM. In the present context, the NP operators contribute to this decay via a diagram similar to Fig. 2, but with $\overline{\nu}\ell$ replaced by $\bar{c}s$ in the final state. The resulting effective Lagrangian would be very similar to Eq. (8), which could lead to effects in the measurement of $\sin(2\beta)$ [19]. We do not consider such effects further here.

Although we do not perform any model calculations in this work, it is worthwhile to consider which types of models could give rise to the various NP operators. The terms in Eqs. (3) and (4) arise in models that contain new charged vector or scalar bosons. For example, extensions of the SM containing gauge bosons with left- and right-handed charged-current couplings (such as the Left-Right Model) would contribute terms such as those appearing in $\mathcal{L}^V_{\rm eff}$ – including the $\mathcal{R}^V_{LR}$ and $\mathcal{R}^V_{RL}$ terms if there were some amount of mixing between the left- and right-handed gauge bosons. Models containing charged scalars (such as the charged Higgs bosons that appear in many extensions of the SM) could give rise to the terms in the expression for $\mathcal{L}^S_{\rm eff}$. Alternatively, there are many FCNC models containing a heavy neutral NP particle (such as a Z' or a neutral Higgs boson) with flavour-changing t-c couplings. Here Fierz rearrangements of the eight operator combinations $(\gamma_\mu P_{L,R})\,[\gamma^\mu P_{L,R}]$ and $(P_{L,R})\,[P_{L,R}]$ (in the notation employed in Ref. [20]) lead to all ten of the operator combinations in Eqs. (3)-(5). In this case there would be mismatched colour indices between the NP and SM diagrams. Appendix C explains how to deal with this situation.

In the following sections we compute various observables associated with the decays $t \to b\bar{b}c$ and $\bar{t} \to \bar{b}b\bar{c}$. We take as our starting point the expressions for the SM and NP amplitudes in Eqs. (1) and (7), respectively.

III. CP-EVEN OBSERVABLES

We begin by considering three CP-even observables associated with the decays in question. The first is the CP-averaged partial width, normalized to the SM result; the second is a

forward-backward-like asymmetry; and the third is a CP-even asymmetry that employs the spin of the top quark. In Secs. III A-III C we work out expressions for the various observables. Section III D contains a numerical analysis and discussion of the results.

A. CP-averaged partial width

We first consider the partial width for $t \to b\bar{b}c$. The expression for the differential partial width, including the various NP terms from the effective Lagrangian, may be found in Eq. (A1) in Appendix A. Performing the integrations over $\rho^2 = (p_t - p_c)^2 = (p_{\bar{b}} + p_b)^2$ and q^2, we find,

$$\begin{aligned}\Gamma\left(t \to b\bar{b}c\right) \simeq \Gamma_{\rm SM}\left(t \to b\bar{b}c\right) \Bigg\{ & 1 + \frac{4\Gamma_W}{m_W}\left[-0.04 \times \mathrm{Re}\left(X_{LL}^{V*}\right) + \mathrm{Im}\left(X_{LL}^{V*}\right)\right] \\ & + \frac{3G_F m_t^2}{\sqrt{2}\pi^2\left(1-\zeta_W^2\right)^2\left(1+2\zeta_W^2\right)}\Bigg[\left|X_{LL}^V\right|^2 + \left|X_{LR}^V\right|^2 + \left|X_{RL}^V\right|^2 + \left|X_{RR}^V\right|^2 \\ & + \frac{1}{4}\left(\left|X_{LL}^S\right|^2 + \left|X_{LR}^S\right|^2 + \left|X_{RL}^S\right|^2 + \left|X_{RR}^S\right|^2\right) + 24\left|X_T\right|^2 + 96\left|X_{TE}\right|^2\Bigg]\Bigg\}, \end{aligned} \tag{12}$$

where $\zeta_W \equiv m_W/m_t$ and

$$\Gamma_{\rm SM}\left(t \to b\bar{b}c\right) \simeq \frac{G_F m_t^3}{24\sqrt{2}\pi}\left(V_{tb}V_{cb}\right)^2\left(1-\zeta_W^2\right)^2\left(1+2\zeta_W^2\right). \tag{13}$$

In calculating the expressions in Eqs. (12) and (13), we have used the narrow width approximation, in which $|G_T(q^2)|^2$ is replaced by a δ-function in q^2, appropriately normalized. [One exception is the term proportional to $\mathrm{Re}(X_{LL}^{V*})$ in Eq. (12), which was computed numerically.]

(Note that the term proportional to $\mathrm{Im}(X_{LL}^{V*})$ in Eq. (12), which is involved in the partial rate asymmetry discussed below, is not quite complete. In its present form, it would lead to a violation of CPT. To avoid running into problems with the CPT theorem, certain vertex-type corrections need to be included in the calculation when computing partial rate asymmetries. We discuss these extra terms in Appendix B.)

The partial width for the CP-conjugate decay may be obtained from Eq. (12) by complex conjugating all weak phases.[1] This has the effect of changing the sign of the $\mathrm{Im}(X_{LL}^{V*})$ term, while leaving the other terms unchanged. Adding the widths for $t \to b\bar{b}c$ and $\bar{t} \to \bar{b}b\bar{c}$, and

[1] Note that the "i" multiplying X_{TE} in the NP amplitude does *not* get complex conjugated when computing the amplitude for the CP-conjugate process.

dividing by twice the SM result yields

$$\begin{aligned}\mathcal{R} &\equiv \frac{\Gamma+\overline{\Gamma}}{2\Gamma_{\rm SM}} \\ &\simeq 1+0.0845\times\Bigg[-0.05\times{\rm Re}\left(X_{LL}^{V*}\right)+\left|X_{LL}^{V}\right|^2+\left|X_{LR}^{V}\right|^2+\left|X_{RL}^{V}\right|^2+\left|X_{RR}^{V}\right|^2 \\ &\quad+\frac{1}{4}\left(\left|X_{LL}^{S}\right|^2+\left|X_{LR}^{S}\right|^2+\left|X_{RL}^{S}\right|^2+\left|X_{RR}^{S}\right|^2\right)+24\left|X_T\right|^2+96\left|X_{TE}\right|^2\Bigg], \qquad (14)\end{aligned}$$

in which we have inserted the known values for the various physical constants, and used the expression for Γ_W noted below Eq. (1). Note that, in practice, the term proportional to ${\rm Re}(X_{LL}^{V*})$ is always small compared to the other terms.

Above, we noted that the X's could well be $O(1)$. Thus, from Eq. (14), we see that the CP-averaged partial width could be used as a tool to search for NP. In particular, an experimental value for $\mathcal{R}$ that is different from unity would give clear evidence for NP. (Depending on the size of the NP signal, it may be important to include corrections to Eq. (13) [21].)

On the other hand, all 10 NP operators contribute to $\mathcal{R}$ in similar ways. Thus, even if the measurement of $\mathcal{R}$ reveals the presence of NP, it does not give us any clue as to the type of NP. For this reason, it is important to look for signs of NP in other quantities. This is most easily done using observables that are strictly zero within the context of the SM. Such observables would typically depend upon differing combinations of NP parameters, so that the observation of NP effects using several different observables would yield insight into the precise nature of the NP. In the following, we construct several asymmetries that are zero within the context of the SM and discuss their potential usefulness as tools for searching for NP.

Note that the ratio $\mathcal{R}$, defined above, will also appear in the denominators of all asymmetries considered below. Since $\mathcal{R}$ is primarily a sum of positive quantities, and since it will always appear in the denominators of the asymmetries, it will always tend to decrease the values of the asymmetries compared to the analogous expressions employing the approximation $\mathcal{R}\approx 1$.

B. Forward-Backward-Like Asymmetry

A tool that has historically been useful to experimentalists is the forward-backward (FB) asymmetry. The differential width for $t \to b\bar{b}c$ may be written in terms of $q^2 = (p_t - p_b)^2 = (p_{\bar{b}} + p_c)^2$ and $\cos\theta$, where θ is the angle between the momentum of the top quark and that of the charm quark in the $\bar{b}$-c rest frame. The FB asymmetry makes use of the following asymmetric integration over $\cos\theta$,

$$\Gamma_{\rm FB} = \int_0^{m_t^2} \left[\int_0^1 \frac{d\Gamma}{dq^2\, d\cos\theta} d\cos\theta - \int_{-1}^0 \frac{d\Gamma}{dq^2\, d\cos\theta} d\cos\theta \right] dq^2 \,. \tag{15}$$

We choose instead to work with the kinematical variables q^2 and ρ^2, noting that

$$\cos\theta = \frac{m_t^2 - 2\rho^2 - q^2}{q^2 - m_t^2}, \tag{16}$$

Using Eq. (16), we may rewrite Eq. (15) as follows,

$$\Gamma_{\rm FB} = \int_0^{m_t^2} \left[\int_{\left(m_t^2 - q^2\right)/2}^{m_t^2 - q^2} \frac{d\Gamma}{dq^2 d\rho^2} d\rho^2 - \int_0^{\left(m_t^2 - q^2\right)/2} \frac{d\Gamma}{dq^2 d\rho^2} d\rho^2 \right] dq^2 \,. \tag{17}$$

Let us first consider the SM contribution to the FB asymmetry. The SM-only contribution to the width is such that

$$\frac{d\Gamma_{\rm SM}}{dq^2 d\rho^2} \propto \left| G_T\left(q^2\right) \right|^2 \left(q^2 + \rho^2\right) \left(m_t^2 - q^2 - \rho^2\right) \tag{18}$$

(see Eq. (A1) in Appendix A). Using the integration prescription in Eq. (17), and assuming the narrow-width approximation, we find,

$$A_{\rm FB}^{\rm SM} = \frac{\Gamma_{\rm FB}^{\rm SM} + \overline{\Gamma}_{\rm FB}^{\rm SM}}{\Gamma_{\rm SM} + \overline{\Gamma}_{\rm SM}} = \frac{\Gamma_{\rm FB}^{\rm SM}}{\Gamma_{\rm SM}} \simeq -\frac{3\zeta_W^2}{2\left(1 + 2\zeta_W^2\right)} \simeq -0.228. \tag{19}$$

Thus, we see that the SM contribution to the FB asymmetry is non-zero.

As noted above, in order to use a particular asymmetry as a discriminator of NP, it is useful if the asymmetry is zero when no NP contribution is present. The regular FB asymmetry does not satisfy this requirement, as is evidenced by Eq. (19). It turns out, however, that if we modify the ρ^2 integration prescription somewhat, the SM contribution can be made to disappear. That is, instead of breaking up the integral over ρ^2 at the point $\rho_{\rm FB}^2 = \left(m_t^2 - q^2\right)/2$, as is done in Eq. (17), we move the boundary to the value $\overline{\rho}^2$,

$$\Gamma_{\overline{\rho}^2} \equiv \int_0^{m_t^2} \left[\int_{\overline{\rho}^2}^{m_t^2 - q^2} \frac{d\Gamma}{dq^2 d\rho^2} d\rho^2 - \int_0^{\overline{\rho}^2} \frac{d\Gamma}{dq^2 d\rho^2} d\rho^2 \right] dq^2 \,, \tag{20}$$

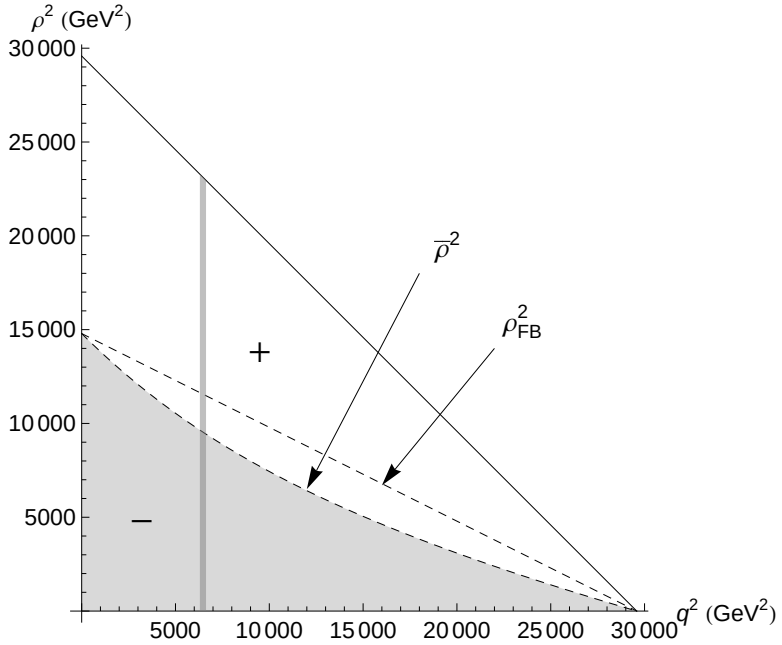

FIG. 3: Phase space for $t \to b\bar{b}c$. The gray vertical bar shows the location of the W resonance at $q^2 = m_W^2$. The shaded and clear regions (separated by the curve denoted "$\overline{\rho}^2$") are used in the construction of the FB-like asymmetry $A_{\overline{\rho}^2}$. The line indicated by "$\rho^2_{\rm FB}$" shows the boundary used in the usual definition of the FB asymmetry.

in which $\overline{\rho}^2$ is chosen such that [see Eq. (18)],

$$\int_0^{\overline{\rho}^2} \left(q^2+\rho^2\right)\left(m_t^2-q^2-\rho^2\right) d\rho^2 = \int_{\overline{\rho}^2}^{m_t^2-q^2} \left(q^2+\rho^2\right)\left(m_t^2-q^2-\rho^2\right) d\rho^2. \tag{21}$$

Then, by construction,

$$\Gamma^{\rm SM}_{\overline{\rho}^2} = \int_0^{m_t^2} \left[\int_{\overline{\rho}^2}^{m_t^2-q^2} \frac{d\Gamma_{\rm SM}}{dq^2 d\rho^2} d\rho^2 - \int_0^{\overline{\rho}^2} \frac{d\Gamma_{\rm SM}}{dq^2 d\rho^2} d\rho^2 \right] dq^2 = 0. \tag{22}$$

The new boundary, $\overline{\rho}^2$, is q^2-dependent and can be solved for numerically.[2] Figure 3 shows the phase space available for $t \to b\bar{b}c$ and also indicates the two boundary choices described above. The vertical band indicates the location of the W resonance for the SM contribution.

Equation (A1) in Appendix A gives the expression for $d\Gamma/dq^2 d\rho^2$. The ρ^2 dependence of the SM piece is given by $(q^2+\rho^2)\,(m_t^2-q^2-\rho^2)$; the SM-NP cross terms and the $\left|X^V_{LL}\right|^2$ and

[2] The equation for $\overline{\rho}^2$ is cubic and can also be solved analytically, although the resulting expressions for the roots of the equation are not particularly enlightening.

$\left|X^V_{RR}\right|^2$ terms have this same ρ^2 dependence. Since the integration prescription described above is engineered to eliminate the SM term when integrating over ρ^2, these latter terms also disappear upon integration over ρ^2 in this manner. Performing the integration numerically for the other terms yields the following,

$$\begin{aligned}\Gamma_{\overline{\rho}^2} \;\simeq\; & \frac{3G_F^2 m_t^5 \left(V_{tb}V_{cb}\right)^2}{16\pi^3}\Bigg[0.155\left(\left|X^V_{LR}\right|^2+\left|X^V_{RL}\right|^2\right) \\ & +0.0208\left(\left|X^S_{LL}\right|^2+\left|X^S_{RR}\right|^2+\left|X^S_{LR}\right|^2+\left|X^S_{RL}\right|^2\right) \\ & +0.310\,\mathrm{Re}\left[X_T\left(X^{S*}_{LL}+X^{S*}_{RR}\right)-2X_{TE}\left(X^{S*}_{LL}-X^{S*}_{RR}\right)\right] \\ & +1.81\left(\left|X_T\right|^2+4\left|X_{TE}\right|^2\right)\Bigg]. \end{aligned} \tag{23}$$

The above expression is CP-even; i.e., the analogous expression for $\bar{t}\to\bar{b}b\bar{c}$ is the same. Finally, we form an FB-like asymmetry as follows,

$$\begin{aligned}A_{\overline{\rho}^2}=\frac{\Gamma_{\overline{\rho}^2}+\overline{\Gamma}_{\overline{\rho}^2}}{\Gamma+\overline{\Gamma}} \;\simeq\; & \frac{1}{\mathcal{R}}\Bigg[0.0393\left(\left|X^V_{LR}\right|^2+\left|X^V_{RL}\right|^2\right) \\ & +0.00528\left(\left|X^S_{LL}\right|^2+\left|X^S_{RR}\right|^2+\left|X^S_{LR}\right|^2+\left|X^S_{RL}\right|^2\right) \\ & +0.0786\,\mathrm{Re}\left[X_T\left(X^{S*}_{LL}+X^{S*}_{RR}\right)-2X_{TE}\left(X^{S*}_{LL}-X^{S*}_{RR}\right)\right] \\ & +0.460\left(\left|X_T\right|^2+4\left|X_{TE}\right|^2\right)\Bigg]. \end{aligned} \tag{24}$$

By construction, this asymmetry is only non-zero if NP contributions are present. Section III D contains a discussion of the range of sizes that are possible for the FB-like asymmetry. At this point we note only that asymmetries of order tens of percent are possible.

C. CP-even Spin Asymmetry

The final CP-even observable that we consider depends on the spin of the top quark [22]. We construct this asymmetry in such a way that it will be zero in the SM and potentially non-zero in the context of NP. Equation (A2) in Appendix A contains the expression for the absolute value squared of the total amplitude, keeping only those terms that contain the top-quark spin four-vector. The term proportional to $\left|G_T\right|^2$ in that expression is the SM contribution. The next term [proportional to $\mathrm{Re}\big(G_T X^{V*}_{LL}\big)$] arises from the interference of the SM contribution with one of the NP terms. The remaining terms are purely NP in origin. Inspection of Eq. (A2) reveals that the SM term is proportional to $p_{\overline{b}}\cdot s_t$. (This is

related to the fact that, in the SM, the spin of the top is in the direction of the momentum of the $\bar{b}$ in the top's rest frame [23].) Working in the top rest frame, we define

$$\vec{s}_{\parallel,\pm} = \pm \frac{1}{\sin\theta_{\bar{b}c}} \left(\widehat{n}_c - \widehat{n}_{\bar{b}} \cos\theta_{\bar{b}c}\right) , \tag{25}$$

where $\widehat{n}_{\bar{b}(c)} = \vec{p}_{\bar{b}(c)}/|\vec{p}_{\bar{b}(c)}|$ and where $\theta_{\bar{b}c}$ is the angle (assumed to be between 0 and π) between the three-momentum of the $\bar{b}$ and that of the c, in the top's rest frame. The cosine and sine of this angle are given, respectively, by,

$$\begin{aligned} \cos\theta_{\bar{b}c} &= \frac{m_t^2\left(\rho^2 - q^2\right) - \rho^2\left(\rho^2 + q^2\right)}{\left(m_t^2 - \rho^2\right)\left(\rho^2 + q^2\right)}, \\ \sin\theta_{\bar{b}c} &= \frac{2m_t\sqrt{\rho^2 q^2\left(m_t^2 - q^2 - \rho^2\right)}}{\left(m_t^2 - \rho^2\right)\left(\rho^2 + q^2\right)}. \end{aligned} \tag{26}$$

The vectors $\vec{s}_{\parallel,\pm}$ are in the decay plane and are perpendicular to $\vec{p}_{\bar{b}}$ by construction. Setting $s^\mu_{t,\pm} = \left(0, \vec{s}_{\parallel,\pm}\right)$, we then have $p_{\bar{b}} \cdot s_{t,\pm} = 0$. Thus, the SM contribution to the amplitude squared disappears for these orientations of the top quark's spin. We can thus construct an asymmetry based on this spin configuration that will be zero within the SM, making it potentially a sensitive probe for NP. We first define,

$$\Gamma_\parallel \equiv \frac{1}{2}\left[\Gamma\left(\vec{s}_{\parallel,+}\right) - \Gamma\left(\vec{s}_{\parallel,-}\right)\right], \tag{27}$$

where the factor of "1/2" is to account for the average over the top quark's spins. Using Eqs. (A2), (25) and (26), and incorporating the integration over phase space, we obtain,

$$\begin{aligned} \Gamma_\parallel &= \frac{G_F^2 m_t^5 \left(V_{tb}V_{cb}\right)^2}{70\pi^2}\Bigg\{ \left(\left|X^V_{LR}\right|^2 - \left|X^V_{RL}\right|^2\right) \\ &\quad -\frac{1}{4}\left(\left|X^S_{LL}\right|^2 - \left|X^S_{RR}\right|^2 + \left|X^S_{LR}\right|^2 - \left|X^S_{RL}\right|^2\right) \\ &\quad +2\,\mathrm{Re}\left[X_T\left(X^{S*}_{LL} - X^{S*}_{RR}\right) - 2X_{TE}\left(X^{S*}_{LL} + X^{S*}_{RR}\right)\right] - 96\,\mathrm{Re}[X_T X^*_{TE}]\Bigg\}. \end{aligned} \tag{28}$$

Finally, summing over the process and the CP-conjugate process, we obtain,

$$\begin{aligned} A_\parallel &= \frac{\Gamma_\parallel + \overline{\Gamma}_\parallel}{\Gamma + \overline{\Gamma}} \\ &\simeq \frac{0.0607}{\mathcal{R}}\Bigg\{ \left(\left|X^V_{LR}\right|^2 - \left|X^V_{RL}\right|^2\right) - \frac{1}{4}\left(\left|X^S_{LL}\right|^2 - \left|X^S_{RR}\right|^2 + \left|X^S_{LR}\right|^2 - \left|X^S_{RL}\right|^2\right) \\ &\quad +2\,\mathrm{Re}\left[X_T\left(X^{S*}_{LL} - X^{S*}_{RR}\right) - 2X_{TE}\left(X^{S*}_{LL} + X^{S*}_{RR}\right)\right] - 96\,\mathrm{Re}[X_T X^*_{TE}]\Bigg\}, \end{aligned} \tag{29}$$

where we have used the fact that $12\sqrt{2}G_F m_t^2/[35\pi(1-\zeta_W^2)^2(1+2\zeta_W^2)] \simeq 0.0607$. A discussion of numerical values obtainable for the CP-even single-spin asymmetry follows in the next subsection.

D. Discussion of CP-even Observables

In this section we have described three observables that are even under CP and that could be used to detect the presence of NP in the decays $t \to b\bar{b}c$ and $\bar{t} \to \bar{b}b\bar{c}$. Should NP be discovered, detailed analysis of such observables could allow experimentalists to map out the nature of the NP.

The first observable considered in this section was a ratio, $\mathcal{R}$, which was defined to be proportional to the CP-averaged partial width. Of the observables considered in this work, $\mathcal{R}$ would probably be the simplest to measure experimentally. Decisive experimental deviation from the SM value $\mathcal{R} = 1$ would be evidence for NP.

On the other hand, $\mathcal{R}$ cannot be used to distinguish the different NP operators. To do this requires the use of other quantities. It is useful to employ observables that give a null signal within the context of the SM. For such observables, a significant departure from zero would be a "smoking-gun" signal for new physics. In addition, since they depend differently on the various NP operators, the observation of non-zero values for these observables would help in identifying the type of NP.

The usual forward-backward asymmetry for $t \to b\bar{b}c$ is expected to be non-zero within the context of the SM. It is possible, however, to alter the kinematical weighting that is used in defining the FB asymmetry in such a way that the resulting "FB-like" asymmetry is zero within the context of the SM. Equation (24) defines the FB-like asymmetry $A_{\bar{\rho}^2}$ in terms of an asymmetric integration over the kinematical variable ρ^2. The integration is engineered in such a way that the SM contribution disappears kinematically. In Eq. (29) we formed a CP-even asymmetry using the spin of the top quark. This asymmetry was also defined in such a way that it was zero within the context of the SM. A non-zero experimental signal for either of these asymmetries would indicate the presence of NP.

Table I contains some representative values for the CP-even asymmetries $A_{\bar{\rho}^2}$ and $A_{\parallel}$, along with the corresponding value for the ratio $\mathcal{R}$ in each case. The entries in the table are ordered from smaller $\mathcal{R}$ values in the top rows to larger ones in the bottom rows. As is evident from the table, when $\mathcal{R}$ is close to unity (meaning that it may not be a very clear discriminator of NP), it is still possible to have CP-even asymmetries that are on the order of several percent. For larger $\mathcal{R}$ values, the asymmetries $A_{\bar{\rho}^2}$ and $A_{\parallel}$ can reach into the 10's of percent. Note, however, that there are some NP scenarios in which $A_{\parallel}$ suffers

TABLE I: Some representative values for the FB-like asymmetry $A_{\bar{\rho}^2}$ and the CP-even spin asymmetry $A_\parallel$. The value for $\mathcal{R}$ is also included for each case.

X^V_{LR}	X^V_{RL}	X^S_{LL}	X^S_{LR}	X^S_{RL}	X^S_{RR}	X_T	X_{TE}	$\mathcal{R}$	$A_{\bar{\rho}^2}$	$A_\parallel$
1.5								1.2	7.4%	11%
				2.5	2.5			1.3	5.2%	15%
		1			−1	0.5	0.125	1.7	6.9%	−14%
		1			−1	0.5	−0.125	1.7	12%	29%
		−2.5			2.5		0.25	1.8	21%	0%
						0.5	−0.25	2.0	11%	36%
2.5	2.5							2.1	24%	0%
						1		3.0	15%	0%
		2.5			2.5	1		3.3	28%	0%

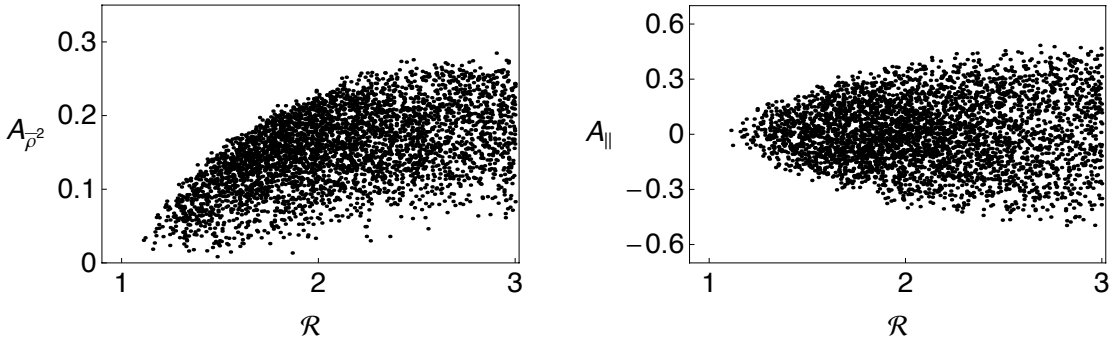

FIG. 4: Scatter plots of the CP-even asymmetries $A_{\bar{\rho}^2}$ and $A_\parallel$ for various combinations of the NP parameters.

cancellations or is zero, even if the NP parameters themselves are non-zero. For example, if $\left|X^V_{LR}\right| = \left|X^V_{RL}\right|$, the contributions from these two parameters cancel in $A_\parallel$.

The CP-even observables are displayed in another manner in Fig. 4, which shows scatter plots of $A_{\bar{\rho}^2}$ versus $\mathcal{R}$ and $A_\parallel$ versus $\mathcal{R}$. The points in this plot were obtained by generating real random numbers for eight of the ten NP parameters over various ranges. (X^V_{LL} and X^V_{RR} were excluded, since they do not contribute to the numerator of either asymmetry.) Asymmetries were only plotted if $\mathcal{R} \leq 3$. Again, it is evident that CP-even asymmetries of order a few 10's of percent are possible.

IV. CP-ODD OBSERVABLES

In addition to the CP-even observables considered in the previous section, it is also possible to construct CP-odd observables related to the decay $t \to b\bar{b}c$. In this section we consider two such observables. The first is the partial rate asymmetry, which compares the partial width for the process to that of the CP-conjugate process. The second is a triple-product asymmetry, which is formed using the spin of the top quark and the three-momenta of two of the final-state quarks. To be non-zero, both of these asymmetries require the presence of at least two contributing amplitudes with a non-trivial relative weak phase. Let us first consider the partial rate asymmetry.

A. Partial Rate Asymmetry

The SM amplitude for $t \to b\bar{b}c$ is dominated by a single contribution. As such, the partial rate asymmetry vanishes. In the presence of NP, the partial-rate asymmetry (PRA) can be nonzero if there is a NP contribution to the decay with a relative weak phase. As can be seen in Eq. (12), there is one important NP piece of this type – X_{LL}^V. The contribution to the PRA then comes from the interference of the SM W-exchange amplitude with the X_{LL}^V term. What we see in this subsection is that the PRA can actually be of order several percent if the Lorentz structure of the NP is $(V-A)\times(V-A)$.

We have noted above that a non-zero PRA requires the interference of at least two amplitudes having a non-zero relative weak phase. Another requirement is that these amplitudes have a non-zero relative strong phase. Strong phases can come from the exchange of gluons, but they can also emerge from the imaginary parts of loop diagrams that do not involve gluons. In particular, if an exchanged particle in the process has a resonance, there is a strong phase associated with the width of that particle. Strong phases originating from particles' widths have been used to generate PRAs in many different systems, including $t \to b\bar{b}c$ [2, 24], $t \to b\tau^+\nu$ [2, 4–7, 9], and various supersymmetric decays [25–27]. In the present calculation, the width of the W provides the required strong phase. This means that the PRA can only arise from SM-NP interference, since NP-NP interference terms do not have a relative strong phase.

Using the expression in Eq. (12), and recalling that the analogous expression for the

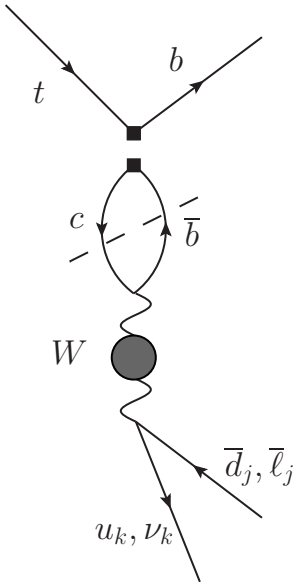

FIG. 5: Vertex correction-type diagrams involving the effective operators shown in Fig. 1 (b). These diagrams contribute to the cancellations required by the CPT theorem. The dashed line indicates that only the absorptive parts of the diagrams are computed.

CP-conjugate process involves the complex conjugation of the weak phases, we immediately find the following expression for the partial rate asymmetry,

$$A_{\rm CP} = \frac{\Gamma - \overline{\Gamma}}{\Gamma + \overline{\Gamma}} \simeq \frac{1}{\mathcal{R}} \frac{4\Gamma_W}{m_W} {\rm Im}\left(X_{LL}^{V*}\right) \simeq \frac{0.102}{\mathcal{R}} \times {\rm Im}\left(X_{LL}^{V*}\right). \tag{30}$$

As was noted above, the PRA requires the existence of a non-zero relative strong phase between interfering amplitudes. In this example, the strong phase is provided by the width of the W, which is the reason that the PRA is proportional to Γ_W. Examination of Eq. (30) reveals that the best-case scenario for the PRA occurs when X_{LL}^V is purely imaginary, or nearly so, and all other NP coefficients are zero. In this case, $\mathcal{R} \simeq 1 + 0.0845 \left|X_{LL}^V\right|^2$, and we find that the PRA is maximized when $\left|X_{LL}^V\right| \simeq 3.44$. The maximum possible PRA, obtained in this manner, is approximately 18%.

As is well-known [28, 29], the CPT theorem requires that we actually be a bit more careful when computing PRAs. In particular, invariance under CPT requires that the total width of the top be equal to that of the anti-top. Our result in Eq. (30) shows that, under certain circumstances, the *partial* width for $t \to b\bar{b}c$ is not equal to the partial width for $\overline{t} \to \overline{b}b\overline{c}$. This necessarily implies that there must be compensating partial rate asymmetries in other

top/anti-top decay modes such that the total top width is still equal to the total anti-top width. In order to respect CPT in this way, it turns out that we need to include another class of diagrams, shown in Fig. 5. These diagrams contribute to various top decay modes, inducing partial rate asymmetries in these modes in such a way that the total top width is equal to the total anti-top width. In the special case $t \to b\bar{b}c$, the effect is such that "Γ_W" in the numerator of Eq. (30) gets replaced by "$\Gamma_W - \Gamma\left(W \to \bar{b}c\right)$" [24, 30, 31], which is to say that the strong phase due to the rescattering process $W \to \bar{b}c \to W$ does not contribute to the PRA. Since $\Gamma\left(W \to \bar{b}c\right)$ is very small, we may safely neglect its effect. It is worthwhile to explore this point a bit further, however, and we do so in Appendix B. Specifically, we verify that the diagrams in Fig. 5 interfere with their SM counterparts in such a way that the CPT theorem is respected, and we also comment on the PRAs that result in other decay modes due to the NP effective operators for $t \to b\bar{b}c$.

B. Triple Product Asymmetry

Mathematically, triple-product asymmetries (TPAs) in $t \to b\bar{b}c$ are related to terms of the form $\vec{v}_i \cdot (\vec{v}_j \times \vec{v}_k)$ in the absolute value squared of the amplitude, where each of the $\vec{v}_i$ could represent a momentum or spin. Working in the rest frame of the top quark, there are only two independent three-momenta. Thus, in order to obtain a non-zero TPA, we need to include one or more spins in $\vec{v}_i \cdot (\vec{v}_j \times \vec{v}_k)$. Since the light final-state quarks hadronize, it is difficult to gain useful information from their spins. The situation is different for the top quark, however, since it decays too quickly to hadronize. In this case, we can construct asymmetries based on $\vec{s} \cdot (\vec{p}_1 \times \vec{p}_2)$, where $\vec{s}$ is the top quark's spin and $\vec{p}_1$ and $\vec{p}_2$ are two of the final-state momenta [32]. In the context of the calculation, these terms arise from expressions such as $\epsilon_{\alpha\beta\gamma\delta} p_t^\alpha s_t^\beta p_{\bar{b}}^\gamma p_c^\delta$.

Now, the PRA considered above contained a factor of $\Gamma_W \sim 2$ GeV in the numerator. The presence of this factor was due to the requirement that there be a relative strong phase between diagrams contributing to the PRA. On the other hand, TPAs do not require a strong phase and are thus not suppressed by a factor of Γ_W. This means that TPAs could in principle be much larger than the PRA considered above. As we shall see, there are in fact certain NP operators that can produce a large TPA.

Because TPAs are CP-odd quantities, they require a non-zero relative weak phase between

interfering diagrams, just as the PRA did. But because no strong phase is necessary, TPAs can in principle arise both from SM-NP and NP-NP interference. (Due to the strong phase requirement, the PRA could only arise from SM-NP interference.) What we find, however, is that the only TPA that survives is one due to NP-NP interference.

All triple-product terms in the absolute value squared of the amplitude may be written in terms of $\epsilon_{\alpha\beta\gamma\delta} p_t^\alpha s_t^\beta p_{\bar{b}}^\gamma p_c^\delta$. Keeping only such terms, we find the following expression in the rest frame of the top quark,

$$\begin{aligned}
&\frac{1}{3}\sum_{\text{colours}}\sum_{b,\bar{b},c\text{ spins}} |\mathcal{M}|^2\big|_{\text{TP}} \\
&= 1536 G_F^2 m_t^2 \left(V_{tb}V_{cb}\right)^2 \vec{s}\cdot(\vec{p}_{\bar{b}}\times\vec{p}_c)\,\text{Im}\big[X_T\big(X_{LL}^{S*}+X_{RR}^{S*}\big)-2X_{TE}\big(X_{LL}^{S*}-X_{RR}^{S*}\big)\big], \qquad (31)
\end{aligned}$$

in which $\vec{s}$ denotes the top's spin [see also Eq. (A2)]. In computing the above expression, we have summed over quark colours and over the final-state quarks' spins, and have divided by 3 for the average over the top quark's colours. Setting

$$\vec{s}_{\perp,\pm} = \pm\frac{\vec{p}_{\bar{b}}\times\vec{p}_c}{|\vec{p}_{\bar{b}}\times\vec{p}_c|}, \qquad (32)$$

we define

$$\Gamma_{\text{TP}} \equiv \frac{1}{2}\left[\Gamma\left(\vec{s}_{\perp,+}\right) - \Gamma\left(\vec{s}_{\perp,-}\right)\right], \qquad (33)$$

where the factor of "1/2" is to account for the average over the top quark's spins. Using the result in Eq. (31) and incorporating the integration over phase space, we obtain,

$$\Gamma_{\text{TP}} = \frac{2G_F^2 m_t^5 \left(V_{tb}V_{cb}\right)^2}{35\pi^2}\text{Im}\big[X_T\left(X_{LL}^{S*}+X_{RR}^{S*}\right)-2X_{TE}\left(X_{LL}^{S*}-X_{RR}^{S*}\right)\big], \qquad (34)$$

in which we have used the fact that

$$|\vec{p}_{\bar{b}}\times\vec{p}_c| = \frac{1}{2m_t}\left[q^2\rho^2\left(m_t^2-q^2-\rho^2\right)\right]^{1/2}\ . \qquad (35)$$

Finally, we define the TPA as

$$A_{\text{CP}}^{\text{TP}} \equiv \frac{\Gamma_{\text{TP}}-\overline{\Gamma}_{\text{TP}}}{\Gamma+\overline{\Gamma}}, \qquad (36)$$

so that

$$\begin{aligned}
A_{\text{CP}}^{\text{TP}} &\simeq \frac{1}{\mathcal{R}}\frac{48\sqrt{2}G_F m_t^2}{35\pi}\frac{\text{Im}\big[X_T\left(X_{LL}^{S*}+X_{RR}^{S*}\right)-2X_{TE}\left(X_{LL}^{S*}-X_{RR}^{S*}\right)\big]}{\left(1-\zeta_W^2\right)^2\left(1+2\zeta_W^2\right)} \\
&\simeq \frac{0.243}{\mathcal{R}}\,\text{Im}\big[X_T\left(X_{LL}^{S*}+X_{RR}^{S*}\right)-2X_{TE}\left(X_{LL}^{S*}-X_{RR}^{S*}\right)\big]. \qquad (37)
\end{aligned}$$

TABLE II: Some representative values for the triple-product asymmetry. The second to last column also shows $\mathcal{R}$ for each case.

X^S_{LL}	X^S_{RR}	X_T	X_{TE}	$\mathcal{R}$	$A_{\rm CP}^{\rm TP}$
$-1.5i$	$-1.5i$	0.5	0	1.6	23%
$2.5i$	$-2.5i$	0	0.4	2.6	38%
$-2.5i$	$-2.5i$	1	0	3.3	37%

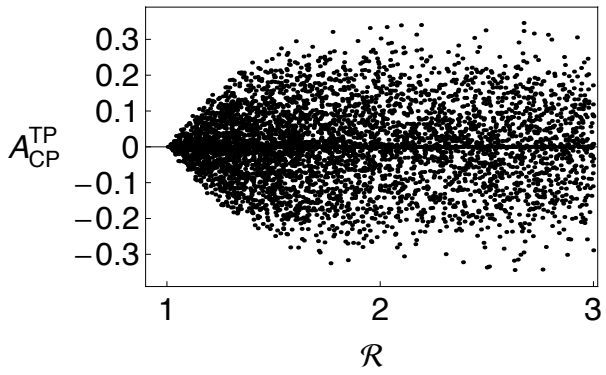

FIG. 6: Scatter plot of the CP-odd TP asymmetry $A_{\rm CP}^{\rm TP}$ for various combinations of the NP parameters.

Table II contains some numerical results following from the above expression, showing that the TPAs can indeed be large – of order 10's of percent – if the NP coefficients are assumed not to be suppressed. Figure 6 shows a scatter plot of $A_{\rm CP}^{\rm TP}$ versus $\mathcal{R}$. The points in this plot were obtained by generating combinations of purely real and purely imaginary random numbers for X^S_{LL}, X^S_{RR}, X_T and X_{TE} over various ranges. Once again, asymmetries were only plotted if $\mathcal{R} \leq 3$. It is evident from the plot that relatively large TPAs are possible.

V. DISCUSSION AND CONCLUSIONS

In this paper we consider new-physics (NP) contributions to the decay $t \to b\bar{b}c$. In the Standard Model (SM), this is a tree-level process: $t \to bW \to b\bar{b}c$. However, the SM amplitude involves the small Cabibbo-Kobayashi-Maskawa element V_{cb} ($\simeq 0.04$), and is therefore suppressed. As a result, the decay is quite sensitive to NP. Rather than working within the context of any one particular extension of the SM, we parameterize the NP

couplings by an effective Lagrangian that includes the 10 possible four-Fermi operators. We show that the SM and NP contributions to $t \to b\bar{b}c$ can indeed be about the same size.

We first compute the $t \to b\bar{b}c$ partial width in the presence of NP. The ratio $\mathcal{R}$, defined in Eq. (14), provides a quantitative measure of the deviation of the partial width from its SM expectation ($\mathcal{R} = 1$ in the SM). This shows clearly that this observable is excellent for showing that NP is present – significant deviations of $\mathcal{R}$ from 1 are possible.

On the other hand, the partial width is not a good observable to *identify* the new physics – all 10 NP operators contribute to $\mathcal{R}$ in a similar way. In order to get an idea of the type of NP present, it is necessary to consider other quantities. To this end, we construct two CP-conserving and two CP-violating observables: (i) CP-even: a forward-backward-like asymmetry [$A_{\bar{p}^2}$ – Eq. (24)] and a top-quark-spin-dependent asymmetry [$A_{\|}$ – Eq. (29)], (ii) CP-odd: the partial rate asymmetry [$A_{\rm CP}$ – Eq. (30)] and a triple-product asymmetry [$A_{\rm CP}^{\rm TP}$ – Eq. (37)]. In each case, the observable is formulated in such a way that it is zero within the context of the SM. The key point is that these observables depend on differing combinations of the NP parameters. This gives them different sensitivities to the various Lorentz structures present in the NP effective Lagrangian.

The allowed values of these four observables vary greatly depending on the values of the NP parameters, but results in the 10-20% range are possible (see Tables I and II). If NP is present, it may well produce measurable values of these observables. Taken together, the measurements of these quantities will give a good indication of the type of NP present.

Acknowledgments: We would like to thank A. Soni for helpful discussions. This work was financially supported by NSERC of Canada (D.L.) The work of K.K., T.K. and K.W. was supported by the U.S. National Science Foundation under Grant PHY–0900914. This work was also partially supported by ANPCyT (Argentina) under grant # PICT-PRH 2009-0054.

Appendix A: Useful Expressions for $t \to b\bar{b}c$

This Appendix contains two expressions that are used to compute observables in the main body of the paper. We take $m_b = m_c \simeq 0$. The first of these is the expression for the partial differential decay width for $t \to \bar{b}bc$. Using Eqs. (1) and (7) and averaging over the

top quark's spins and colours, we find the following,

$$\begin{aligned}
\frac{d\Gamma}{dq^2 d\rho^2} = \frac{3G_F^2 \left(V_{tb}V_{cb}\right)^2}{2\left(2\pi\right)^3 m_t^3}\Bigg\{ & \left(q^2+\rho^2\right)\left(m_t^2-q^2-\rho^2\right) \\
& \times\left[m_W^4\left|G_T\right|^2 + 4m_W^2\,\mathrm{Re}\left(G_T X_{LL}^{V*}\right) + 4\left(\left|X_{LL}^V\right|^2+\left|X_{RR}^V\right|^2\right)\right] \\
& + 4\rho^2\left(m_t^2-\rho^2\right)\left(\left|X_{LR}^V\right|^2+\left|X_{RL}^V\right|^2\right) \\
& + q^2\left(m_t^2-q^2\right)\left(\left|X_{LL}^S\right|^2+\left|X_{RR}^S\right|^2+\left|X_{LR}^S\right|^2+\left|X_{RL}^S\right|^2\right) \\
& + 8q^2\left(-m_t^2+q^2+2\rho^2\right)\mathrm{Re}\left[X_T\left(X_{LL}^{S*}+X_{RR}^{S*}\right)-2X_{TE}\left(X_{LL}^{S*}-X_{RR}^{S*}\right)\right] \\
& + 32\left[m_t^2\left(q^2+4\rho^2\right)-\left(q^2+2\rho^2\right)^2\right]\left(\left|X_T\right|^2+4\left|X_{TE}\right|^2\right)\Bigg\},
\end{aligned} \tag{A1}$$

in which V_{tb} and V_{cb} have been taken to be real. The analogous expression for $\bar{t}\to\bar{b}b\bar{c}$ is obtained by complex conjugating all of the NP coefficients (X_{LL}^V, etc.), while leaving G_T unchanged.

It is also useful to have the expression for the absolute value squared of the amplitude, keeping only the terms that contain the spin four vector for the top quark. This expression is used to compute the CP-even single-spin asymmetry in Sec. III C and the TP asymmetry in Sec. IV B. Keeping only terms containing the spin four vector of the top quark, we find,

$$\begin{aligned}
& \frac{1}{3}\sum_{\text{colours}}\sum_{b,\bar{b},c\text{ spins}}\left|\mathcal{M}\right|^2\Big|_{s_t} \\
& = 96G_F^2 m_t\left(V_{tb}V_{cb}\right)^2\Bigg\{\left(m_t^2-q^2-\rho^2\right)\Bigg[-m_W^4\left|G_T\right|^2-4m_W^2\,\mathrm{Re}\left(G_T X_{LL}^{V*}\right) \\
& - 4\left(\left|X_{LL}^V\right|^2-\left|X_{RR}^V\right|^2\right)\Bigg]p_{\bar{b}}\cdot s_t - 4\rho^2\left(\left|X_{LR}^V\right|^2-\left|X_{RL}^V\right|^2\right)p_c\cdot s_t \\
& - q^2\left(\left|X_{LL}^S\right|^2-\left|X_{RR}^S\right|^2+\left|X_{LR}^S\right|^2-\left|X_{RL}^S\right|^2\right)p_b\cdot s_t \\
& + 8\,\mathrm{Re}\left[X_T\left(X_{LL}^{S*}-X_{RR}^{S*}\right)-2X_{TE}\left(X_{LL}^{S*}+X_{RR}^{S*}\right)\right]\left[\left(m_t^2-q^2\right)p_{\bar{b}}\cdot s_t+\rho^2 p_b\cdot s_t\right] \\
& + 128\,\mathrm{Re}\left[X_T X_{TE}^*\right]\left[\left(2m_t^2-q^2-2\rho^2\right)p_{\bar{b}}\cdot s_t+\left(q^2+2\rho^2\right)p_c\cdot s_t\right] \\
& - 16\,\mathrm{Im}\left[X_T\left(X_{LL}^{S*}+X_{RR}^{S*}\right)-2X_{TE}\left(X_{LL}^{S*}-X_{RR}^{S*}\right)\right]\epsilon\left(p_t,s_t,p_{\bar{b}},p_c\right)\Bigg\},
\end{aligned} \tag{A2}$$

in which s_t denotes the top's spin four vector and $\epsilon\left(p_t,s_t,p_{\bar{b}},p_c\right)\equiv\epsilon_{\alpha\beta\gamma\delta}p_t^\alpha s_t^\beta p_{\bar{b}}^\gamma p_c^\delta$. In writing the above expression, we have used the fact that $p_t\cdot s_t=0$. We have also summed over quark colours and over the final-state quarks' spins, and have divided by 3 for the average over the top quark's colours.

Appendix B: CPT and Beyond

The CPT theorem requires the total decay width for the top to be equal to that for the anti-top. An apparent violation of the CPT theorem arises, however, if the NP contributions in Fig. 1 (b) are the only ones that are kept. That this is the case is straightforward to see, since the diagram in Fig. 1 (b) affects the partial widths for $t \to b\bar{b}c$ and $\bar{t} \to \bar{b}b\bar{c}$ differently [leading to the PRA in Eq. (30)], but has no effect on the other top or anti-top decay modes. Thus, the top and anti-top total widths are not equal if only such contributions are kept, resulting in an apparent violation of the CPT theorem. This phenomenon is well-known (see, for example, Refs. [7, 24, 28–31]). In this Appendix we show that the inclusion of certain vertex-type corrections gives rise to compensating differences in the top and anti-top widths. The sum of the differences is zero, so that the top and anti-top widths no longer differ, in agreement with the CPT theorem.

Let us define the partial width difference for the decay $t \to b\bar{j}k$ as follows,

$$\Delta\Gamma\left(t \to b\bar{j}k\right) \equiv \Gamma\left(t \to b\bar{j}k\right) - \Gamma\left(\bar{t} \to \bar{b}j\bar{k}\right), \tag{B1}$$

in which j and k could refer either to quarks or to leptons. For the case $t \to b\bar{b}c$, the main contribution to $\Delta\Gamma$ is due to the interference between the SM and NP diagrams indicated in Fig. 1. Another important set of contributions for the decay $t \to b\bar{j}k$ is indicated in Fig. 5. The absorptive parts of these vertex-like corrections interfere with their associated SM diagrams in such a way that the conservation of CPT is manifest. Using the Cutkosky rules to calculate the absorptive part of the vertex-like corrections, we find

$$\Delta\Gamma\left(t \to b\bar{j}k\right) \simeq \frac{2\sqrt{2}G_F m_W^2 \left(V_{cb}\right)^2}{\pi} \mathrm{Im}\big(X_{LL}^{V*}\big)\Gamma\left(t \to bW\right)\big[\delta_{\bar{j}\bar{b}}\delta_{kc} - \mathcal{B}\left(W \to \bar{j}k\right)\big]. \tag{B2}$$

Summing over $\bar{j}$ and k (including both quark and lepton final states), we have

$$\sum_{\bar{j},k} \Delta\Gamma\left(t \to b\bar{j}k\right) = 0, \tag{B3}$$

demonstrating that the CPT theorem is indeed respected once the absorptive parts of the diagrams in Fig. 5 are included.

Equation (B2) gives a correction to the PRA for $t \to b\bar{b}c$, leading to the following modification of Eq. (30),

$$A_{\mathrm{CP}} \simeq 0.102 \times \frac{\mathrm{Im}\left(X_{LL}^{V*}\right)}{\mathcal{R}}\left[1 - \mathcal{B}\left(W \to \bar{b}c\right)\right]. \tag{B4}$$

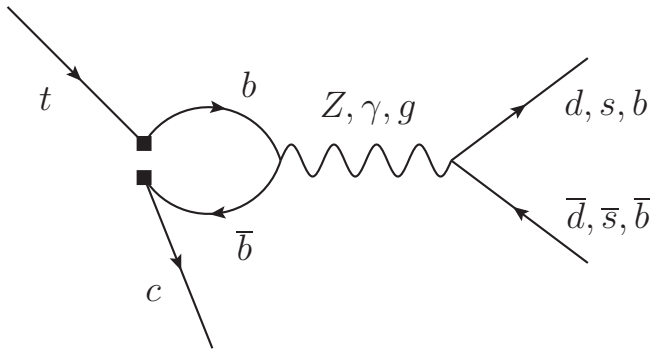

FIG. 7: A loop-level contribution of the NP operators that could contribute to PRAs in $t \to f\overline{f}c$, with $f = d, s, b$.

The correction to the original expression is miniscule, since $\mathcal{B}\left(W \to \bar{b}c\right) \simeq |V_{cb}|^2/3 \simeq 5.5 \times 10^{-4}$.

An interesting consequence of the CPT theorem is that, if NP operators give a PRA in a particular decay mode (such as $t \to b\bar{b}c$, as in our case), then those same NP operators must also contribute to one or more other decay modes in such a way that the total width of the top is the same as that of the anti-top. This means that those other decay modes must also have PRAs (barring other accidental cancellations). We can use Eq. (B2) to estimate the PRAs in other decay modes due to the NP operators in Eqs. (3)-(5). The resulting expression is given by,

$$A_{\rm CP}\big(t \to b\bar{j}k\big) \simeq -\frac{\sqrt{2}G_F m_W^2 (V_{cb})^2}{\pi} {\rm Im}\big(X_{LL}^{V*}\big) \simeq -5.6 \times 10^{-5}\, {\rm Im}\big(X_{LL}^{V*}\big)\,,\ \bar{j}k \neq \bar{b}c. \qquad \text{(B5)}$$

Thus the contributions of these NP operators to PRAs in other top decay modes are expected to be very small. One could also consider the complementary question: Are there NP operators, other than those given in Eqs. (3)-(5), that could contribute to the PRA in $t \to b\bar{b}c$? The answer to this question appears to be yes. For example, the effective operators $(\bar{s}\,\mathcal{O}_1 c)(\bar{c}\,\mathcal{O}_2 b)$ or $\big(\bar{d}\,\mathcal{O}_1 u\big)(\bar{c}\,\mathcal{O}_2 b)$ could appear in a diagram similar to that in Fig. 5, but with the usual SM tbW vertex at the top, and the NP-induced one-loop correction to the Wbc vertex at the bottom. Such operators are constrained by B decays.

We should note that the NP effective operators in Eqs. (3)-(5) give rise to other loop-level diagrams that could contribute to PRAs in top decays. The contributions in different decay modes would still complement each other in the sense that the total top and anti-top

widths would remain equal. Figure 7 shows an example of loop-level corrections to $t \to f\overline{f}c$ ($f = d, s, b$) mediated by the NP operators considered in this work. These diagrams could interfere with their corresponding SM diagrams to induce PRAs. We do not compute such contributions here.

Appendix C: Effect of Including Colour-mismatched Terms

The effective Lagrangian incorporating NP effects given in Eqs. (3)-(5) assumed that the colour indices contracted in the same manner as those of the SM diagram. This need not be the case, so it is useful to consider the effects of including colour-mismatched terms in the effective Lagrangian. To this end, let us generalize the NP effective Lagrangian in Eq. (3) as follows,

$$\begin{aligned}\mathcal{L}^V_{\rm eff} \;=\; \frac{g'^2}{M^2}\,\{&\mathcal{R}^V_{LL}\,\overline{b}_a\gamma_\mu P_L t_a\,\overline{c}_b\gamma^\mu P_L b_b + \mathcal{R}^{V\prime}_{LL}\,\overline{b}_a\gamma_\mu P_L t_b\,\overline{c}_b\gamma^\mu P_L b_a \\ &+\mathcal{R}^V_{LR}\,\overline{b}_a\gamma_\mu P_L t_a\,\overline{c}_b\gamma^\mu P_R b_b + \mathcal{R}^{V\prime}_{LR}\,\overline{b}_a\gamma_\mu P_L t_b\,\overline{c}_b\gamma^\mu P_R b_a \\ &+\ldots\} + \text{h.c.},\end{aligned} \tag{C1}$$

and similarly for Eqs. (4) and (5). In this expression, the subscripts a and b are colour indices and the primed coefficients correspond to the new, colour-mismatched terms. The total amplitude for $t_a \to b_b\overline{b}_c c_d$ (with the subscripts a, b, c and d representing the colours) could then be parameterized as

$$\mathcal{M}_{abcd} = \sum_i \left(\mathbb{R}_i\delta_{ab}\delta_{cd} + \mathbb{R}'_i\delta_{ad}\delta_{bc}\right)\mathcal{M}_i\,, \tag{C2}$$

in which the sum runs over the SM diagram, plus all NP contributions. The factors $\mathbb{R}_i$ and $\mathbb{R}'_i$ are the coefficients for the colour-matched and colour-mismatched terms, respectively, and are assumed to contain all of the weak phases. (The $\mathbb{R}'$ coefficient for the SM term is assumed to be zero.) For a given value of i, the phases of $\mathbb{R}_i$ and $\mathbb{R}'_i$ could be different. The factors $\mathcal{M}_i$ contain all the spinors and γ matrices and, in the case of the SM diagram, the W propagator.

Summing over the quarks' colours and dividing by 3 for the average over the top quark's colours, we find,

$$\frac{1}{3}\sum_{a,b,c,d}\mathcal{M}_{abcd}\mathcal{M}^*_{abcd} \;=\; 3\sum_i\left[|\mathbb{R}_i|^2 + |\mathbb{R}'_i|^2 + \frac{2}{3}\,\text{Re}(\mathbb{R}_i\mathbb{R}'^*_i)\right]|\mathcal{M}_i|^2$$

$$+\ 6\sum_{j>i}\left\{\mathrm{Re}\left[\mathbb{R}_i\mathbb{R}_j^* + \mathbb{R}_i'\mathbb{R}_j'^* + \frac{1}{3}\left(\mathbb{R}_i\mathbb{R}_j'^* + \mathbb{R}_i'\mathbb{R}_j^*\right)\right]\mathrm{Re}\big(\mathcal{M}_i\mathcal{M}_j^*\big)\right.$$
$$\left. -\ \mathrm{Im}\left[\mathbb{R}_i\mathbb{R}_j^* + \mathbb{R}_i'\mathbb{R}_j'^* + \frac{1}{3}\left(\mathbb{R}_i\mathbb{R}_j'^* + \mathbb{R}_i'\mathbb{R}_j^*\right)\right]\mathrm{Im}\big(\mathcal{M}_i\mathcal{M}_j^*\big)\right\}. \qquad \text{(C3)}$$

The $\mathbb{R}_i\mathbb{R}_j^*$ terms in the above expression correspond to the "colour-matched" terms that we have taken into account in this work. The other terms are new.

Equation (C3) can be used to generalize the expressions in this paper, provided the expressions have already been split cleanly into pieces containing the weak phases ($\mathbb{R}_i$, etc.) and those containing the spinors and any strong phases ($\mathcal{M}_i$). Expressions containing SM-NP cross-terms may safely set $\mathbb{R}_{\rm SM} = 1$ and incorporate the entire amplitude into the "$\mathcal{M}_{\rm SM}$" part [in Eq. (C2)], since V_{tb} and V_{cb} have been taken to be real. As an example, the generalized form for Eq. (14) would be

$$\mathcal{R} \simeq 1 + 0.0845 \times \left[-0.05 \times \mathrm{Re}\left(X_{LL}^{V*} + \frac{1}{3}X_{LL}^{V\prime *}\right) \right.$$
$$\left. + \left|X_{LL}^{V}\right|^2 + \left|X_{LL}^{V\prime}\right|^2 + \frac{2}{3}\mathrm{Re}\left(X_{LL}^{V}X_{LL}^{V\prime *}\right) + \ldots \right], \qquad \text{(C4)}$$

in which we have used the fact that $\mathbb{R}'_{\rm SM} = 0$. Similarly, Eq. (37) would become,

$$A_{\rm CP}^{\rm TP} \simeq \frac{0.243}{\mathcal{R}}\,\mathrm{Im}\big\{ X_T\left(X_{LL}^{S*} + X_{RR}^{S*}\right) - 2X_{TE}\left(X_{LL}^{S*} - X_{RR}^{S*}\right)$$
$$+\ X_T'\left(X_{LL}^{S\prime *} + X_{RR}^{S\prime *}\right) - 2X_{TE}'\left(X_{LL}^{S\prime *} - X_{RR}^{S\prime *}\right)$$
$$+\frac{1}{3}\left[X_T\left(X_{LL}^{S\prime *} + X_{RR}^{S\prime *}\right) - 2X_{TE}\left(X_{LL}^{S\prime *} - X_{RR}^{S\prime *}\right)\right.$$
$$\left. +X_T'\left(X_{LL}^{S*} + X_{RR}^{S*}\right) - 2X_{TE}'\left(X_{LL}^{S*} - X_{RR}^{S*}\right)\right]\big\}, \qquad \text{(C5)}$$

and Eq. (30) would become,

$$A_{\rm CP} \simeq \frac{0.102}{\mathcal{R}} \times \mathrm{Im}\left(X_{LL}^{V*} + \frac{1}{3}X_{LL}^{V\prime *}\right). \qquad \text{(C6)}$$

Finally, an expression such as "$\mathrm{Re}\big(G_T X_{LL}^{V*}\big)$" in Eq. (A1), which contains both a strong phase (in G_T) and a weak phase (in X_{LL}^V), first needs to be separated into two pieces using $\mathrm{Re}\,(AB) = \mathrm{Re}(A)\mathrm{Re}(B) - \mathrm{Im}(A)\mathrm{Im}(B)$.

---

[1] G. Eilam, J. L. Hewett and A. Soni, Phys. Rev. D **44**, 1473 (1991) [Erratum-ibid. D **59**, 039901 (1999)]; M. E. Luke and M. J. Savage, Phys. Lett. B **307**, 387 (1993) [arXiv:hep-ph/9303249];

T. Han, R. D. Peccei and X. Zhang, Nucl. Phys. B **454**, 527 (1995) [arXiv:hep-ph/9506461]; T. Han, K. Whisnant, B. L. Young and X. Zhang, Phys. Rev. D **55**, 7241 (1997) [arXiv:hep-ph/9603247]; T. Han, K. Whisnant, B. L. Young and X. Zhang, Phys. Lett. B **385**, 311 (1996) [arXiv:hep-ph/9606231]; G. Eilam, A. Gemintern, T. Han, J. M. Yang and X. Zhang, Phys. Lett. B **510**, 227 (2001) [arXiv:hep-ph/0102037]; J. A. Aguilar-Saavedra, Acta Phys. Polon. B **35**, 2695 (2004) [arXiv:hep-ph/0409342]; A. Datta and M. Duraisamy, Phys. Rev. D **81**, 074008 (2010) [arXiv:0912.4785 [hep-ph]].

[2] J. L. Diaz-Cruz and G. Lopez Castro, Phys. Lett. B **301**, 405 (1993).

[3] D. Atwood, G. Eilam, A. Soni, R. R. Mendel and R. Migneron, Phys. Rev. Lett. **70**, 1364 (1993); D. Atwood, G. Eilam and A. Soni, Phys. Rev. Lett. **71**, 492 (1993) [arXiv:hep-ph/9303268].

[4] R. Cruz, B. Grzadkowski and J. F. Gunion, Phys. Lett. B **289**, 440 (1992).

[5] J. Liu, Phys. Rev. D **47**, 1741 (1993) [arXiv:hep-ph/9209294].

[6] D. Atwood, G. Eilam, A. Soni, R. R. Mendel and R. Migneron, Phys. Rev. D **49**, 289 (1994).

[7] T. Arens and L. M. Sehgal, Phys. Rev. D **51**, 3525 (1995) [arXiv:hep-ph/9404259].

[8] X. J. Bi and Y. B. Dai, Eur. Phys. J. C **12**, 125 (2000) [arXiv:hep-ph/9904228].

[9] D. Atwood, S. Bar-Shalom, G. Eilam and A. Soni, Phys. Rept. **347**, 1 (2001) [arXiv:hep-ph/0006032].

[10] B. Grzadkowski and W. Y. Keung, Phys. Lett. B **319**, 526 (1993) [arXiv:hep-ph/9310286]; E. Christova and M. Fabbrichesi, Phys. Lett. B **320**, 299 (1994) [arXiv:hep-ph/9307298]; S. Bar-Shalom, D. Atwood and A. Soni, Phys. Rev. D **57**, 1495 (1998) [arXiv:hep-ph/9708357].

[11] M. Nowakowski and A. Pilaftsis, Z. Phys. C **60**, 121 (1993) [arXiv:hep-ph/9305321].

[12] G. López Castro, J. L. Lucio and J. Pestieau, Int. J. Mod. Phys. A **11**, 563 (1996) [arXiv:hep-ph/9504351].

[13] J. Papavassiliou and A. Pilaftsis, Phys. Rev. Lett. **75**, 3060 (1995) [arXiv:hep-ph/9506417].

[14] J. Papavassiliou, in *"Beyond the Standard Model IV,"* pp. 509-513, eds. J. Gunion, T. Han and J. Ohnemus (1995) [arXiv:hep-ph/9504386].

[15] D. Binosi and J. Papavassiliou, Phys. Rept. **479**, 1 (2009) [arXiv:0909.2536 [hep-ph]].

[16] C. P. Burgess and D. London, Phys. Rev. D **48**, 4337 (1993) [arXiv:hep-ph/9203216].

[17] K. Nakamura *et al.* [Particle Data Group], J. Phys. G **37**, 075021 (2010).

[18] G. H. Wu, K. Kiers and J. N. Ng, Phys. Rev. D **56**, 5413 (1997) [arXiv:hep-ph/9705293].

[19] K. Kiers, A. Soni and G. H. Wu, Phys. Rev. D **59**, 096001 (1999) [arXiv:hep-ph/9810552].

[20] C. C. Nishi, Am. J. Phys. **73**, 1160 (2005) [arXiv:hep-ph/0412245].

[21] For a discussion of some corrections to the tree-level result, see W. Bernreuther, J. Phys. G **35**, 083001 (2008) [arXiv:0805.1333 [hep-ph]], and references therein. The effect of the higher-order corrections is to reduce the value of the top width somewhat.

[22] For a discussion of top quark polarization, see M. Beneke, I. Efthymiopoulos, M. L. Mangano, J. Womersley, A. Ahmadov, G. Azuelos, U. Baur, A. Belyaev *et al.*, [hep-ph/0003033], and references therein.

[23] D. Atwood, A. Aeppli, A. Soni, Phys. Rev. Lett. **69**, 2754-2757 (1992).

[24] G. Eilam, J. L. Hewett and A. Soni, Phys. Rev. Lett. **67**, 1979 (1991).

[25] K. Kiers, A. Szynkman and D. London, Phys. Rev. D **74**, 035004 (2006) [arXiv:hep-ph/0605123].

[26] A. Szynkman, K. Kiers and D. London, Phys. Rev. D **75**, 075009 (2007) [arXiv:hep-ph/0701165].

[27] M. Nagashima, K. Kiers, A. Szynkman, D. London, J. Hanchey and K. Little, Phys. Rev. D **80**, 095012 (2009) [arXiv:0907.1063 [hep-ph]].

[28] J. M. Gerard and W. S. Hou, Phys. Rev. Lett. **62**, 855 (1989).

[29] L. Wolfenstein, Phys. Rev. D **43**, 151 (1991).

[30] J. M. Soares, Phys. Rev. Lett. **68**, 2102 (1992).

[31] G. Eilam, J. L. Hewett and A. Soni, Phys. Rev. Lett. **68**, 2103 (1992).

[32] For a similar discussion in the context of $t \to b\ell^+\nu$, see G. L. Kane, G. A. Ladinsky and C. P. Yuan, Phys. Rev. D **45**, 124 (1992).